

that can be determined based on the following system of equations, representing measurements from four different satellites:

$$\begin{aligned}\tilde{\rho}^{(1)} = & [(X^{(1)} - x)^2 + (Y^{(1)} - y)^2 + (Z^{(1)} - z)^2]^{0.5} \\ & + c\Delta t_r + c\Delta t_{sv}^{(1)} + c\Delta t_a^{(1)} + SA^{(1)} + E^{(1)} + MP^{(1)} + \eta^{(1)}\end{aligned}\quad (5.1)$$

$$\begin{aligned}\tilde{\rho}^{(2)} = & [(X^{(2)} - x)^2 + (Y^{(2)} - y)^2 + (Z^{(2)} - z)^2]^{0.5} \\ & + c\Delta t_r + c\Delta t_{sv}^{(2)} + c\Delta t_a^{(2)} + SA^{(2)} + E^{(2)} + MP^{(2)} + \eta^{(2)}\end{aligned}\quad (5.2)$$

$$\begin{aligned}\tilde{\rho}^{(3)} = & [(X^{(3)} - x)^2 + (Y^{(3)} - y)^2 + (Z^{(3)} - z)^2]^{0.5} \\ & + c\Delta t_r + c\Delta t_{sv}^{(3)} + c\Delta t_a^{(3)} + SA^{(3)} + E^{(3)} + MP^{(3)} + \eta^{(3)}\end{aligned}\quad (5.3)$$

$$\begin{aligned}\tilde{\rho}^{(4)} = & [(X^{(4)} - x)^2 + (Y^{(4)} - y)^2 + (Z^{(4)} - z)^2]^{0.5} \\ & + c\Delta t_r + c\Delta t_{sv}^{(4)} + c\Delta t_a^{(4)} + SA^{(4)} + E^{(4)} + MP^{(4)} + \eta^{(4)}\end{aligned}\quad (5.4)$$

where $\tilde{\rho}^{(1)}$, $\tilde{\rho}^{(2)}$, $\tilde{\rho}^{(3)}$, and $\tilde{\rho}^{(4)}$ are the measured pseudoranges, $(X^{(i)}, Y^{(i)}, Z^{(i)})$ are the ECEF position coordinates of satellite i , (x, y, z) are the ECEF position coordinates of the receiver antenna, Δt_r is receiver clock bias, $\Delta t_{sv}^{(i)}$ is the clock bias of the SV, $\Delta t_a^{(i)}$ is the atmospheric delay, $SA^{(i)}$ represents the deliberate corruption of the satellite signals under the policy of selective availability, $E^{(i)}$ represents error in the broadcast ephemeris data, $MP^{(i)}$ represents multipath error, $\eta^{(i)}$ represents receiver tracking error noise, and c is the speed of light. The $()^{(i)}$ notation refers to the quantity in parenthesis referenced to the i th satellite.

Each of the above error sources is discussed separately in Sec. 5.4. In solving Eqs. (5.1)–(5.4), the effective SV positions are required. The position of the space-vehicle antenna phase center in ECEF coordinates can be computed with data derived from the GPS navigation messages, as described in App. E.

5.3 Solution of the Pseudorange Equations

In equations (5.1)–(5.4), the pseudorange measurements are dependent on the receiver coordinates in a nonlinear fashion. Although closed-form solutions are available (see, e.g., Refs. 5, 38, and 97), in this section the typical method of solution, based on linearization of the measurement equations, is presented. This approach is straightforward, converges quickly, and allows linear analysis techniques to be applied. The linearization approaches of this chapter leads into the EKF technique used in later examples. If improved accuracy is desired, the linearization and solution procedure can be repeated iteratively with the result from one iteration serving as the linearization point for the next iteration; however, the more typical approach (for a stationary antenna) is to perform a single iteration for each measurement epoch with the result of one epoch serving as the linearization point for the next epoch. Nonstationary antenna situations are discussed in Chap. 7.

Linearizing Eqs. (5.1)–(5.4) gives

$$\begin{bmatrix} \tilde{\rho}^{(1)}(\mathbf{x}) \\ \tilde{\rho}^{(2)}(\mathbf{x}) \\ \tilde{\rho}^{(3)}(\mathbf{x}) \\ \tilde{\rho}^{(4)}(\mathbf{x}) \end{bmatrix} = \begin{bmatrix} \hat{\rho}^{(1)}(\mathbf{x}_0) \\ \hat{\rho}^{(2)}(\mathbf{x}_0) \\ \hat{\rho}^{(3)}(\mathbf{x}_0) \\ \hat{\rho}^{(4)}(\mathbf{x}_0) \end{bmatrix} + \mathbf{H} \begin{bmatrix} (x - x_0) \\ (y - y_0) \\ (z - z_0) \\ c\Delta t_r \end{bmatrix} + \begin{bmatrix} \chi^{(1)} \\ \chi^{(2)} \\ \chi^{(3)} \\ \chi^{(4)} \end{bmatrix} + \text{hot's} \quad (5.5)$$

where $\chi^{(i)}$ has been used as a shorthand to denote the terms $c\Delta t_{sv}^{(i)} + c\Delta t_a^{(i)} + \text{SA}^{(i)} + E^{(i)} + \text{MP}^{(i)} + \eta^{(i)}$ corrupting each measurement, (x_0, y_0, z_0) is the point of linearization, *hot's* represents the higher-order terms in the expansion

$$\rho^{(i)}(\mathbf{x}) = [(X^{(i)} - x)^2 + (Y^{(i)} - y)^2 + (Z^{(i)} - z)^2]^{0.5} \quad (5.6)$$

$$\mathbf{H} = \begin{bmatrix} \frac{\delta\rho^{(1)}}{\delta x} & \frac{\delta\rho^{(1)}}{\delta y} & \frac{\delta\rho^{(1)}}{\delta z} & 1 \\ \frac{\delta\rho^{(2)}}{\delta x} & \frac{\delta\rho^{(2)}}{\delta y} & \frac{\delta\rho^{(2)}}{\delta z} & 1 \\ \frac{\delta\rho^{(3)}}{\delta x} & \frac{\delta\rho^{(3)}}{\delta y} & \frac{\delta\rho^{(3)}}{\delta z} & 1 \\ \frac{\delta\rho^{(4)}}{\delta x} & \frac{\delta\rho^{(4)}}{\delta y} & \frac{\delta\rho^{(4)}}{\delta z} & 1 \end{bmatrix}_{(x_0, y_0, z_0)} \quad (5.7)$$

where

$$\begin{aligned} \frac{\delta\rho^{(i)}}{\delta x} &= \frac{-(X^{(i)} - x)}{[(X^{(i)} - x)^2 + (Y^{(i)} - y)^2 + (Z^{(i)} - z)^2]^{0.5}} \\ \frac{\delta\rho^{(i)}}{\delta y} &= \frac{-(Y^{(i)} - y)}{[(X^{(i)} - x)^2 + (Y^{(i)} - y)^2 + (Z^{(i)} - z)^2]^{0.5}} \\ \frac{\delta\rho^{(i)}}{\delta z} &= \frac{-(Z^{(i)} - z)}{[(X^{(i)} - x)^2 + (Y^{(i)} - y)^2 + (Z^{(i)} - z)^2]^{0.5}} \end{aligned}$$

For a solution, each component of Eq. (5.5) can be written as[†]

$$\delta\hat{\rho}^{(i)} = \tilde{\rho}^{(i)}(\mathbf{x}) - \hat{\rho}^{(i)}(\mathbf{x}_0) = \mathbf{h}^{(i)}\delta\mathbf{x} + \chi^{(i)} + \text{hot's} \quad (5.8)$$

where the first three components of $\mathbf{h}^{(i)}$ (the i th row of \mathbf{H}) form a unit vector pointing from the satellite to \mathbf{x}_0 .

Assuming that the four satellites are selected so that the rows of \mathbf{H} are linearly independent, these four linear equations can be solved by inversion of the \mathbf{H} matrix:

$$\delta\mathbf{x} = \mathbf{H}^{-1} \begin{bmatrix} \delta\hat{\rho}^{(1)} \\ \delta\hat{\rho}^{(2)} \\ \delta\hat{\rho}^{(3)} \\ \delta\hat{\rho}^{(4)} \end{bmatrix} - \mathbf{H}^{-1} \left(\begin{bmatrix} \chi^{(1)} \\ \chi^{(2)} \\ \chi^{(3)} \\ \chi^{(4)} \end{bmatrix} + \text{hot's} \right) \quad (5.9)$$

[†]The measured pseudorange should be corrected for satellite clock offset (Δt_{sv} in App. E).

Since χ is not known, the computed solution is

$$\delta \hat{\mathbf{x}} = \mathbf{H}^{-1} \begin{bmatrix} \delta \hat{\rho}^{(1)} \\ \delta \hat{\rho}^{(2)} \\ \delta \hat{\rho}^{(3)} \\ \delta \hat{\rho}^{(4)} \end{bmatrix} \quad (5.10)$$

with error

$$\mathbf{H}^{-1} \left(\begin{bmatrix} \chi^{(1)} \\ \chi^{(2)} \\ \chi^{(3)} \\ \chi^{(4)} \end{bmatrix} + \text{hot's} \right) \quad (5.11)$$

Although the *hot's* component of the error can be reduced through iteration, the error component due to χ can be reduced only by:

1. PPS implementation, which removes SA and ionospheric error
2. error modeling, possible for atmospheric effects [67], or
3. differential techniques, as discussed in Sec. 5.8.

When measurements from more than four satellites are available, the least-squares solution by Eq. (4.5) is

$$\delta \hat{\mathbf{x}} = (\mathbf{H}^T \mathbf{H})^{-1} \mathbf{H}^T \delta \hat{\rho} \quad (5.12)$$

With knowledge of the position error $\delta \hat{\mathbf{x}}$, the actual position is determined as

$$\hat{\mathbf{x}} = \hat{\mathbf{x}}_0 + \delta \hat{\mathbf{x}}$$

Example At a given time, a set of satellite positions are calculated with the equations in App. E, as shown in Table 5.2. At the corresponding time, the pseudoranges [(transit time Δt_{sv}) c] are measured to be

$$\tilde{\rho}^{(1)}(x) = 22228206.42m$$

$$\tilde{\rho}^{(2)}(x) = 24096139.11m$$

$$\tilde{\rho}^{(3)}(x) = 21729070.63m$$

$$\tilde{\rho}^{(4)}(x) = 21259581.09m$$

What is the receiver location?

TABLE 5.2 Satellite Positions in ECEF Coordinates in Meters

Satellite	x	y	z
SV 2	+7766188.44	-21960535.34	+12522838.56
SV 26	-25922679.66	-6629461.28	+31864.37
SV 4	-5743774.02	-25828319.92	+1692757.72
SV 7	-2786005.69	-15900725.80	+21302003.49

TABLE 5.3 Receiver Position in ECEF Coordinates (meters) as a Function of Iteration Number

k	x	y	z	$c\Delta t_r$
0	0000000.000	0000000.000	0000000.000	000000.000
1	-2977571.476	-5635278.159	4304234.505	162523.980
2	-2451728.534	-4730878.461	3573997.520	314070.732
3	-2430772.219	-4702375.802	3546603.872	264749.706
4	-2430745.096	-4702345.114	3546568.706	264691.129
5	-2430745.096	-4702345.114	3546568.706	264691.129

Assuming no prior position information, the iterative linearization process will be initialized at the ECEF origin. The position-estimation convergence as a function of iteration number is shown in Table 5.3. Note that the estimated position converges to a fixed estimate (to millimeter precision) in five iterations. This does not necessarily mean that the estimated position is accurate to millimeters. In this example, the presurveyed receiver ECEF position in meters is known to be

$$x_0 = -2430829.17 \quad y_0 = -4702341.01 \quad z_0 = +3546604.39$$

At each iteration, the error between the estimated position and the correct position is shown in Table 5.4. This table shows that while the error due to linearization (i.e., *hot's*) has been essentially eliminated, the bias due to the measurement errors remains.

The measurement matrix \mathbf{H} for the last iteration is calculated from Eq. (5.7) to be

$$\mathbf{H} = \begin{bmatrix} -0.4643 & 0.7858 & -0.4087 & 1.0000 \\ 0.9858 & 0.0809 & 0.1475 & 1.0000 \\ 0.1543 & 0.9842 & 0.0864 & 1.0000 \\ 0.0169 & 0.5333 & -0.8457 & 1.0000 \end{bmatrix} \quad (5.13)$$

The inverse of the measurement matrix is

$$\mathbf{H}^{-1} = \begin{bmatrix} -1.9628 & -0.0862 & 1.0122 & 1.0368 \\ -1.7302 & -1.1479 & 2.0344 & 0.8437 \\ 1.1263 & 0.5680 & -0.0604 & -1.6339 \\ 1.9086 & 1.0941 & -1.1533 & -0.8493 \end{bmatrix} \quad (5.14)$$

The first three rows of this inverted measurement matrix (those corresponding to the position estimates) sum to zero. Therefore, if all the measured ranges are biased by

TABLE 5.4 Receiver Position Error in ECEF Coordinates (Meters) as a Function of Iteration Number

k	δx	δy	δz
1	-546742.305	-932937.149	757630.116
2	-20899.364	-28537.451	27393.130
3	56.951	-34.792	-518
4	84.074	-4.104	-35.684
5	84.074	-4.104	-35.684

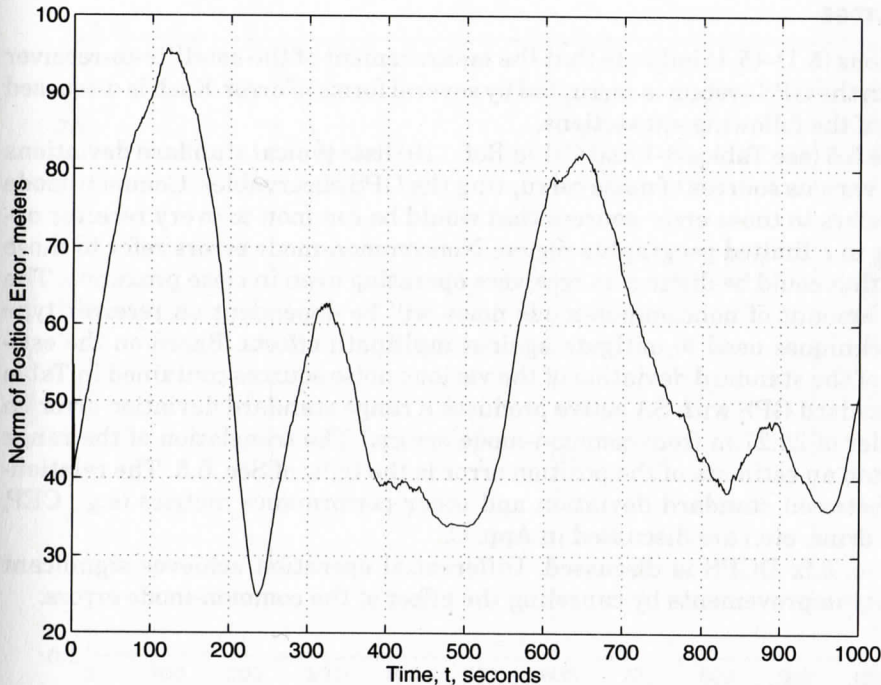


Figure 5.1 Norm of the position error resulting from L1 C/A code processing.

the same amount, the position estimates will be unaffected. The last row, corresponding to the clock bias estimate, sums to one. Therefore any identical bias on all the range measurements appears in the estimate of the clock bias. These two properties will always hold and can be used advantageously in the design of base stations for differential techniques [34].

Figure 5.1 shows the norm of the position estimation error in an L1 C/A code experiment similar to that described in the previous example; again, four satellites are used. For the experiment, the *position dilution of precision* (PDOP; see Sec. 5.5) corresponding to the \mathbf{H} matrix decreased from an initial value of 6.1 to a final value of 4.8. At each time step (1-s intervals), the position estimate is calculated independently by means of least squares. The position-estimate error standard deviations for this particular experiment are [16.29, 27.39, 39.03] m for a circular error probable[†] (CEP) equal to 25.4 m. This figure illustrates the character of the positioning accuracy achievable by SPS GPS. Note that the remaining error is not white, but has significant time correlation. This fact is used advantageously in DGPS systems. The sources and the magnification of these errors are discussed in the next two sections.

[†]Defines the radius of the circle with 50% probability of containing the estimation error, see App. C.